transition-state theory" by knowing only the transition state, its symmetry, and its other usual properties (i.e., frequencies and moments of inertia).

Finally, although it has been emphasized that reaction-path symmetry can induce mode-specific effects between states of different symmetry, without more detailed dynamical calculations there is no way to know that there might not also be mode specificity *within* a given irreducible representation. For the formaldehyde reaction (eq 1.1), for example, it is possible that the rate constant might not be a smooth function of the total energy even within the A' or the A'' manifold. The kind of detailed dynamical calculations that can answer this question have been carried out by Waite and Miller[16] for model problems, and depending on the nature of the coupling one can obtain statistical or mode-specific behavior within a given symmetry. To carry out calculations of this type for the formaldehyde reaction requires the coupling

elements in eq 2.2 and the frequencies along the reaction path that fully characterize the reaction-path Hamiltonian. These quantities have been determined[15] for the formaldehyde dissociation, and calculations for it like those of Waite and Miller are in progress.

(16) B. A. Waite and W. H. Miller, *J. Chem. Phys.*, **73**, 3713 (1980); **74**, 3910 (1981).

(17) B. A. Waite, S. K. Gray, and W. H. Miller, to be published.

Semiconductor Electrodes. 48. Photooxidation of Halides and Water on n-Silicon Protected with Silicide Layers

Fu-Ren F. Fan, R. Gerald Keil, and Allen J. Bard*

Contribution from the Department of Chemistry, University of Texas, Austin, Texas 78712. Received June 14, 1982

Abstract: The electrochemical and photoelectrochemical behavior of n-type silicon electrodes coated with noble metal silicides and RuO_2 in aqueous solutions containing various redox couples was investigated. Iridium silicide coated n-Si electrodes, n-Si(Ir), and RuO_2-modified n-Si(Ir) electrodes can photogenerate I_2, Br_2, and Cl_2 with high stability and efficiencies (>5%). The photooxidation of water on these electrodes is also feasible.

Interest in the stabilization of small band gap n-type semiconductors against photocorrosion in photoelectrochemical (PEC) cells is based on the goal of photogenerating highly oxidizing species (e.g., Br_2, O_2, Cl_2, etc.) on these semiconductor electrodes. Because of its wide use and availability, small band gap n-Si has been of special interest. While naked n-Si is easily photooxidized in aqueous solutions to produce an insulating SiO_2 layer, stable n-Si photoelectrodes can be achieved by coating the photoanode with a thin gold or platinum layer overcoated with a thick polypyrrole film[1j,k] or derivatizing the n-Si surface before coating with a polypyrrole film.[1l] However, the photogeneration of highly oxidizing species, such as Br_2, Cl_2, or O_2, on these electrodes cannot be accomplished because of the instability of polypyrrole in the potential range where the oxidation of Br^-, Cl^-, or H_2O takes place.[2] We have recently demonstrated[3] that Pt silicide coated n-Si electrodes can be employed to fabricate fairly stable PEC

cells with aqueous solutions containing various redox couples, e.g., $Fe^{2+/3+}$, I^-/I_3^-, $Fe(CN)_6^{3-/4-}$.

There is a wealth of information concerning thin-film–semiconductor reactions and the nature of semiconductor/metal interfaces, especially metal thin films on silicon.[4] We report here a study of the electrochemical (EC) and PEC behavior of platinum and iridium silicide coated n-Si electrodes and suitably modified forms of these electrodes in aqueous solutions containing halide ions. We demonstrate that iridium silicide coated n-Si electrodes, denoted n-Si(Ir), and RuO_2-modified n-Si(Ir) electrodes (which are similar to the RuO_2-modified ITO coated n-Si electrodes described recently[1m]) can photogenerate I_2, Br_2, and Cl_2 without noticeable decomposition with efficiencies above 5%. The photooxidation of water is also described.

Experimental Section

Silicides were prepared by procedures similar to those reported previously.[3,4a] n-Si single crystals (0.4–0.6 ohm cm) donated by Texas Instruments were cleaned ultrasonically in trichloroethylene, acetone, and methanol. Immediately prior to vacuum deposition of metal, the n-Si crystals were etched twice with 48% HF solution for 10–20 min. The etched crystals were then rinsed thoroughly with distilled water and methanol and dried under vacuum. The metal films were deposited by flash evaporation of a known amount of metal on the n-Si crystals at a pressure of 10^{-6} torr. The thickness of the metal film deposited on silicon wafers was estimated from the optical density of a metal film deposited

(1) (a) Nakato, Y.; Ohnishi, T.; Tsubomura, H. *Chem. Lett.* **1975**, *19*, 883. (b) Nakato, Y.; Abe, K.; Tsubomura, H. *Ber. Bunsenges. Phys. Chem.* **1976**, *80*, 1002. (c) Kohl, P. A.; Frank, S. N.; Bard, A. J. *J. Electrochem. Soc.* **1977**, *124*, 225. (d) Tomkiewicz, M.; Woodall, J. *Ibid.*, 1436. (e) Noufi, R.; Tench, D.; Warren, L. *Ibid.* **1980**, *127*, 2709, and references therein. (f) Noufi, R.; Frank, A. J.; Nozik, A. J. *J. Am Chem. Soc.* **1981**, *103*, 1849. (g) Bocarsly, A. B.; Walton, E. G.; Wrighton, M. S. *Ibid.* **1980**, *102*, 3390. (h) Bolts, J. M.; Bocarsly, A. B.; Palazzotto, M. C.; Walton, E. G.; Lewis, N. S.; Wrighton, M. S. *Ibid.* **1979**, *101*, 1378. (i) Bolts, J.; Wrighton, M. S. *Ibid.* **1978**, *100*, 5257. (j) Fan, F.-R. F.; Wheeler, B. L.; Bard, A. J.; Noufi, R. *J. Electrochem. Soc.* **1981**, *128*, 2042. (k) Skotheim, T.; Lundstrom, I.; Prejza, J. *Ibid.* 1625. (l) Simon, R. A.; Ricco, J.; Wrighton, M. S. *J. Am. Chem. Soc.* **1982**, *104*, 2031. (m) DuBow, J.; Hodes, G.; Rajeshwar, K., submitted for publication.

(2) (a) Kanazawa, K. K.; Diaz, A. F.; Gill, W. D.; Grant, P. M.; Street, G. B.; Gardini, G. P. *Synth. Met.* **1979/1980**, *1*, 329. (b) Bull, R.; Fan, F.-R. F.; Bard, A. J. *J. Electrochem. Soc.* **1982**, *129*, 1009.

(3) Fan, F.-R. F.; Hope, G.; Bard, A. J., *J. Electrochem. Soc.* **1982**, *129*, 1647.

(4) (a) Tu, K. N.; Mayer, J. W. In "Thin Films--Interdiffusion and Reactions", Poate, J. M., Tu, K. N., Mayer, J. W., Eds.; Wiley: New York, 1978; p 359. (b) Lepselter, M. P.; Andrews, J. M. In "Ohmic Contacts to Semiconductors", Schwartz, B. Ed.; The Electrochemical Society: New York, 1969. (c) Sze, S. M. "Physics of Semiconductor Devices"; Wiley-Interscience: New York, 1969; p 363.
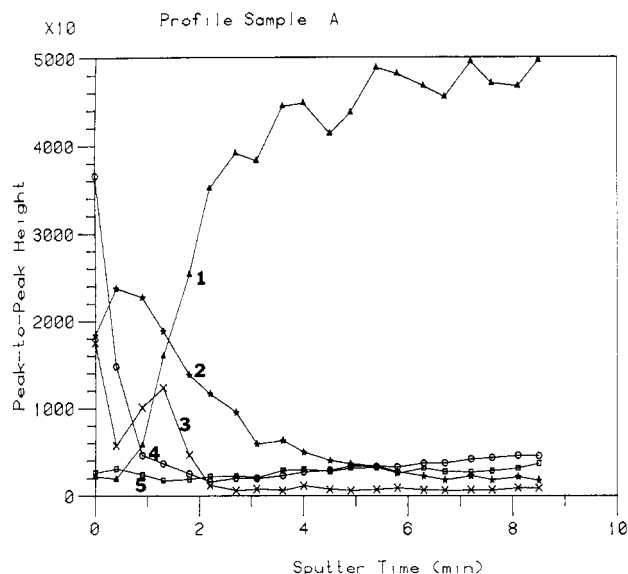
Figure 1. Auger depth profile of a speciment of Pt on Si before thermal annealing. (1) Si; (2) Pt; (3) O; (4) C; (5) W.

Figure 2. Auger depth profile of a specimen of thermally annealed Pt on Si, annealed at ~400 °C and 10^{-6} torr for 30 min. (1) Si; (2) Pt; (3) O; (4) C; (5) W.

on a microscope slide that was placed near the silicon wafers. The optical density of a thicker metal film of known weight was used as the standard, assuming that the density of the metal film is independent of the thickness. The thickness of the metal film was also estimated from the amount of metal placed on the tungsten filament, assuming that the filament was a point evaporating source and the metal was completely and uniformly evaporated in all directions. The results obtained from these two techniques agree within 20% for films <40 Å. Immediately after metal deposition, the metal-coated n-Si crystals were annealed in situ at about 400 °C for 5–30 min, depending on the thickness of the metal film, at a pressure of 10^{-6} torr. The crystals obtained showed a mirrorlike surface with no obvious pits when examined at a magnification of 500X.

RuO$_2$ films were prepared either by dip coating[5] or by spray pyrolysis.[6] Both techniques gave satisfactory results. Dip coating was performed by immersing the silicide-coated silicon substrate for 2 min in 2% (w/w) RuCl$_3$ solution in 2-propanol. This was then dried at 120 °C under N$_2$ for 30 min. A second layer was then deposited in the same way. Pyrolysis was then carried out under O$_2$ in a quartz crucible heated in a tube furnace at 350–400 °C for 1 h. Spray pyrolysis was performed by spraying a 1% RuCl$_3$ solution in 2-propanol on the silicon substrate, which was held at 70 °C. Spray struck the substrate for ~5 s. The film was dried at this temperature for 30 s. Another layer was deposited subsequently. Pyrolysis was then carried out at the same conditions as stated above. A brown uniform film was obtained by both techniques. The Cl$_2$ gas photogenerated was identified and determined by iodometric and gravimetric methods. The photogenerated gaseous products were carried away from the PEC cell with N$_2$ and trapped in three gas purging bottles containing 0.2 M NaI solution. The concentration of iodine produced was determined spectrophotometrically, which gave the total amount of volatile oxidants produced. The excess I⁻ left in the gas washing bottles was then oxidized by the addition of concentrated HNO$_3$ acid. After the I$_2$ was filtered off, the filtrate was heated very gently to remove the dissolved I$_2$. The amount of Cl$_2$ photogenerated was then determined gravimetrically through the precipitation of AgCl.

The detailed procedures for preparing the ohmic contacts and mounting and sealing the electrodes are very similar to those previously reported.[1j] The exposed area of the photoelectrodes ranges from 0.1 to 0.2 cm^2. The voltammetric experiments were performed with the same apparatus and procedures.[7] The light source used in the study of the PEC effect was usually a tungsten–halogen lamp fitted with a 13-cm-thick water filter. AES profile data was obtained by using a Varian Model 981-2707 Auger spectrometer. The samples were analyzed with a 5-keV electron beam probe. A 1-keV argon ion beam was used to sputter the silicide surface. An exact measurement of the silicide film thickness after annealing was not made. However, the experimental conditions under which the silicide was formed produced film thicknesses
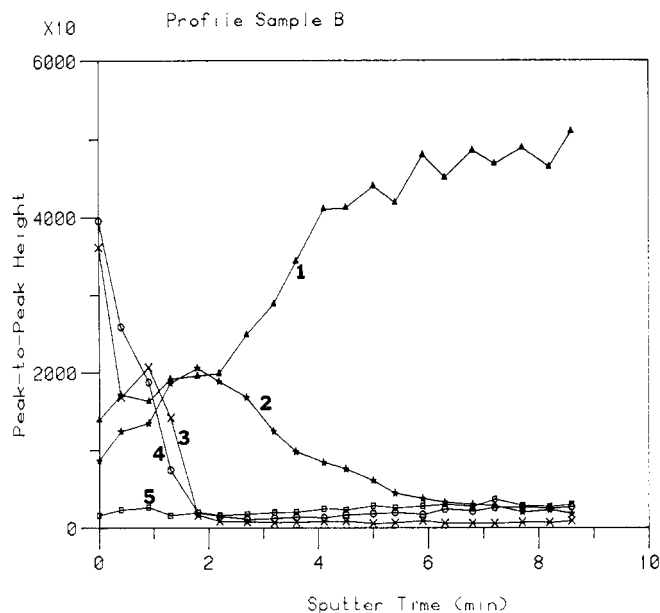
(5) Lodi, G.; Bighi, C.; De Asmundis, C. *Mater. Chem.* **1976**, *1*, 177.

(6) Doblhofer, K.; Metiko, M.; Ogumi, Z.; Gerischer, H. *Ber. Bunsenges. Phys. Chem.* **1978**, *82*, 1046.

(7) Fan, F.-R. F.; White, H. S.; Wheeler, B. L.; Bard, A. J. *J. Am. Chem. Soc.* **1980**, *102*, 5142.

of ~150 Å. Reagent grade chemicals were used without further purification. All solutions were prepared from triply distilled water. All experiments were carried out with the solution under a nitrogen atmosphere. The pH of the solution was adjusted by the addition of concentrated HCl or solid LiOH. Buffer solutions were not used to avoid any complications from oxidtion or reduction of buffer components.

Results and Discussion

Auger Analysis. As shown in Figure 1, the Auger depth profile of Pt on n-Si shows that most of the Pt stayed on the surface before thermal annealing. After annealing in vacuum at 400 °C for about 30 min, there is significant mixing of Pt and Si over a considerable distance (see Figure 2). The atomic ratio of Pt to Si near the surface approaches unity. Oxygen is present in both samples and is concentrated near the surface. Very low levels of tungsten are also found in both samples. This probably arises from simultaneous evaporation of some tungsten–platinum alloy formed on the tungsten filament.

PEC Behavior on PtSi-Coated n-Si Electrodes: n-Si(Pt). The voltammetric curves for an n-Si electrode coated with ~40 Å of Pt and annealed (400 °C at 10^{-6} torr for 10 min) in a solution containing 1 M NaI and 0.1 M iodine is shown in Figure 3. In the dark (curve a), essentially no anodic current is observed while considerable reduction of iodine starts only at potentials negative of 0.0 V vs. SCE.

Under illumination with a light intensity of 65 mW/cm^2 (curve b) net anodic currents are observed at potentials positive of −0.1 V vs. SCE; this represents an open-circuit photovoltage, V_{oc}, of 0.4 V, since the reversible I$_2$/I⁻ potential, estimated by that of a Pt electrode immersed in this solution, is +0.3 V vs. SCE. The short-circuit current density, j_{sc}, was 13 mA/cm^2, and the fill factor was 0.70. The maximum power conversion efficiency was thus 5.6%. As reported previously,[3] fairly stable performance of these photoelectrodes can be achieved in a solution containing the Fe$^{2+/3+}$ couple in a 1 M HCl medium. Similar voltammetric behavior has been obtained in a solution containing Fe(CN)$_6$$^{3-/4-}$, which gives the highest j_{sc} (~20 mA/cm^2 at 65 mW/cm^2) due to less light absorption by the solution.

As shown in Figure 4, in a solution containing 1.0 M NaBr only, the n-Si(Pt) electrodes exhibit no appreciable anodic current in the dark (Figure 4A, curve a). Under irradiation at 40 mW/cm^2, the photooxidation of Br⁻ occurs at potentials positive of 0.4 V vs. SCE (Figure 4A, curve b). The photogeneration of Br$_2$ was easily recognized by the production of an orange-colored stream of Br$_2$ from the electrode surface during illumination and the occurrence of a peak for Br$_2$ reduction on scan reversal. Although

222 *J. Am. Chem. Soc., Vol. 105, No. 2, 1983*

Fan, Keil, and Bard
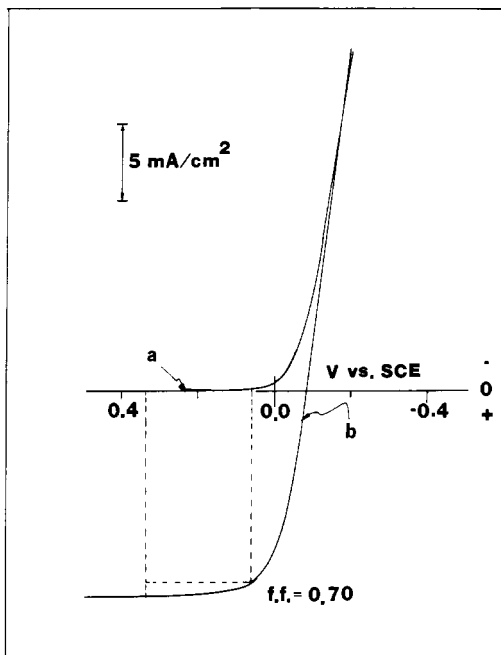
Figure 3. Voltammetric curves of Pt silicide-coated n-Si electrodes in an aqueous solution containing 1.0 M NaI and 0.1 M iodine: (a) in the dark. (b) under illumination of 65 mW/cm² from a tungsten-halogen lamp. Scan rate, 100 mV/s; Pt thickness, ~40 Å annealed at 400 °C and 10⁻⁶ torr for 10 min.
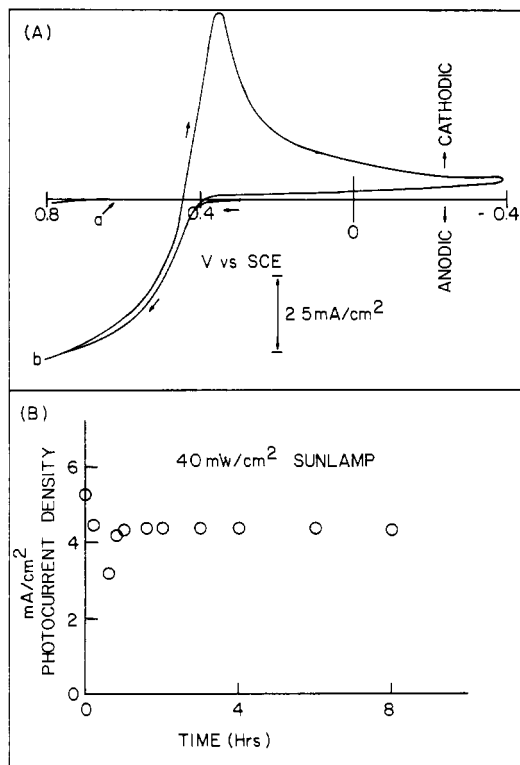

Figure 4. (A) Voltammetric curves of Pt silicide-coated n-Si electrodes in the dark (curve a) and under illumination (curve b) of 40 mW/cm² from a sunlamp. Scan rate, 100 mV/s. The electrolyte solution contains 0.5 M Na_2SO_4 and 1 M NaBr. (B) Photocurrent (at bias potential of 0.8 V vs. SCE) vs. time. Light intensity 40 mW/cm² from a sunlamp. Same electrode and solution as in (A).

these n-Si(Pt) electrodes were not tested for long-term stability, continuous operation with no noticeable decomposition for at least 8 h was obtained (Figure 4B). This represents a substantial improvement in the stability of n-Si photoelectrodes in a corrosive Br_2 medium compared to naked or polypyrrole-coated n-Si
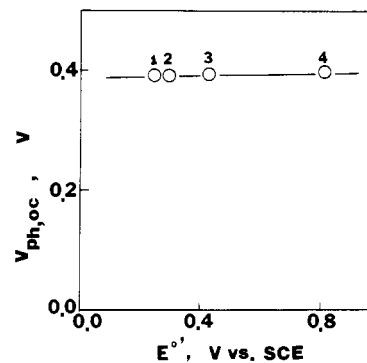

Figure 5. Open-circuit photovoltage vs. the potential of the redox couple on n-Si(Pt) electrodes. Light intensity at 65 mW/cm² (tungsten–halogen lamp). (1) $Fe(CN)_6^{3-/4-}$; (2) I^-/I_3^-; (3) $Fe^{2+/3+}$ (in 1 M HCl); (4) Br^-/Br_2.
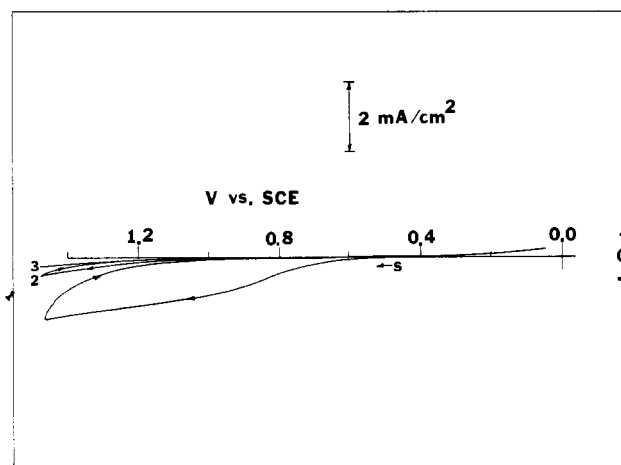

Figure 6. Photovoltammetric curves of n-Si(Pt) electrodes in an 11 M LiCl solution. Light intensity 65 mW/cm²; scan rate 100 mV/cm². The numbers by the curves indicate the number of continuous cycles between the two potential limits.

electrodes. A summary on V_{oc} as a function of the potentials of the redox couples is shown in Figure 5; V_{oc} is essentially independent of the redox potential. As will be described in more detail elsewhere, the origin of the photovoltage is the Schottky barrier formed at the n-Si/PtSi junction. The observed PEC behavior is similar to that found when Fermi level pinning occurs.[8]

While n-Si(Pt) electrodes remain reasonably stable during photooxidation of Br^-, attempts to photooxidize Cl^- in a 11 M LiCl solution result in a significant deterioration of the photocurrent with time (Figure 6).

Photooxidation of Cl^- on n-Si(Ir) Electrodes. Unlike n-Si(Pt) electrodes, iridium silicide coated n-Si electrodes show stable behavior for the photooxidation of Cl^- in 11 M LiCl solution. The voltammetric behavior is shown in Figure 7. In the dark, no appreciable anodic current is observed even at a potential of 1.2 V vs. SCE where rapid Cl_2 evolution occurs on a Pt electrode (curve a). Under illumination at 65 mW/cm², the photooxidation of Cl^- takes place at potentials positive of 0.60 V vs. SCE (curve b). On the reversal scan a cathodic peak is observed, indicating the reduction of the photogenerated Cl_2. The maximum power conversion efficiency at 65 mW/cm², as calculated from curve c in Figure 7, is ~5%. Although n-Si(Ir) electrodes can photooxidize Cl^-, the photoeffect degrades with time (See Figure 11). A sustained photoeffect can be achieved, however, by adding a coating of RuO_2 to the n-Si(Ir) electrodes as illustrated below.

Photooxidation of H_2O and Cl^- on n-Si(Ir)/RuO_2 Electrodes. RuO_2 is known to catalyze Cl_2 and O_2 evolution at electrode surfaces. The voltammetric behavior in 11 M LiCl solution on

(8) Bard, A. J.; Bocarsly, A. B.; Fan, F.-R. F.; Walton, E. G.; Wrighton, M. S. *J. Am. Chem. Soc.* **1980**, *102*, 3671.
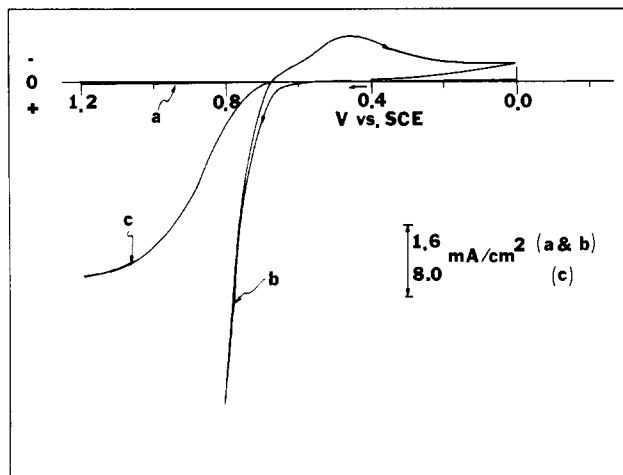
Figure 7. Voltammetric curves of n-Si(Ir) electrodes in 11 M LiCl at pH 5 in the dark (curve a) and under illumination (curves b and c), 65 mW/cm^2 tungsten–halogen lamp. Scan rate 100 mV/s. Curves b and c have different current scales. Ir thickness ~40 Å, annealed at 400 °C and 10^{-6} torr for 10 min.
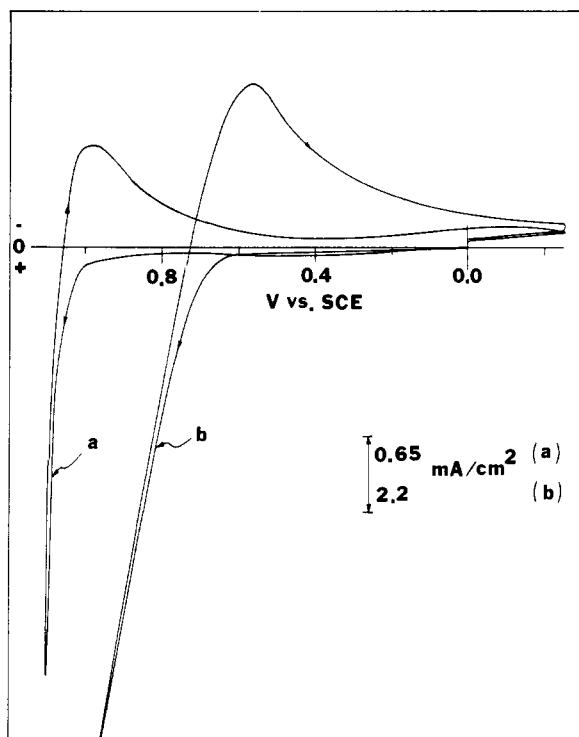

Figure 9. Current–potential curves of n-Si(Ir)/RuO$_2$ electrodes in 1 M NaClO$_4$ in the dark (curve a) and under illumination (curves b and c) with a light intensity of 65 mW/cm^2; scan rate 100 mV/s; b, pH 5; c, pH 13.

Figure 8. Voltammetric curves of Pt (curve a) and n-Si(Ir)/RuO$_2$ (curve b) electrodes in 11 M LiCl at pH 7. Light intensity 65 mW/cm^2; scan rate 100 mV/s.

Figure 10. Current–potential curves of n-Si(Ir)/RuO$_2$ electrodes in 11 M LiCl at different pHs. Light intensity 65 mW/cm^2. (a) pH 1; (b) pH 3; (c) pH 11–12; (d) pH 13.

n-Si(Ir) electrodes with or without an RuO$_2$ coating was very similar. As shown in Figure 8, chlorine evolution occurs at irradiated n-Si(Ir)/RuO$_2$ electrodes at potentials 0.3–0.4 V less positive than at Pt electrodes, which at these current densities operated near the reversible Cl$_2$/Cl$^-$ potential. On the reversal potential scan, a cathodic peak was observed, suggesting that the oxidation product was reduced at this electrode. The same electrode in a 1 M NaClO$_4$ solution also shows a photoanodic current, but no cathodic peak occurs during the reversal scan (Figure 9). The photoanodic current is probably caused by the photooxidation of OH$^-$ or H$_2$O since V_{on} depends strongly on pH and gas bubbles were observed to form on the electrode surface during irradiation.

In 11 M LiCl the voltammetric behavior is strongly pH dependent (Figure 10). At high pH (pH >10), two oxidation waves can be distinguished. The height of the first wave is nearly
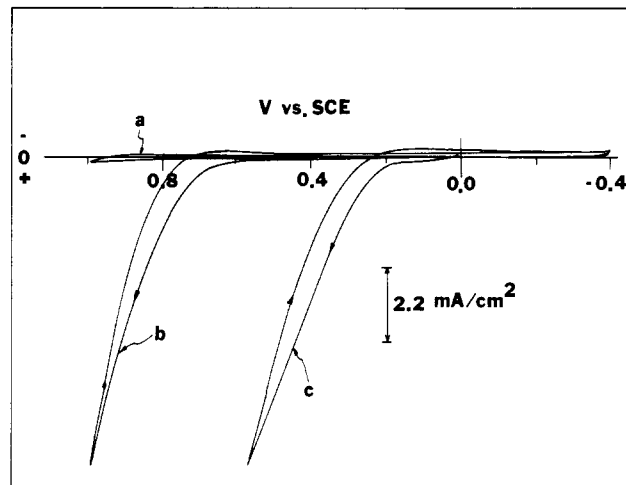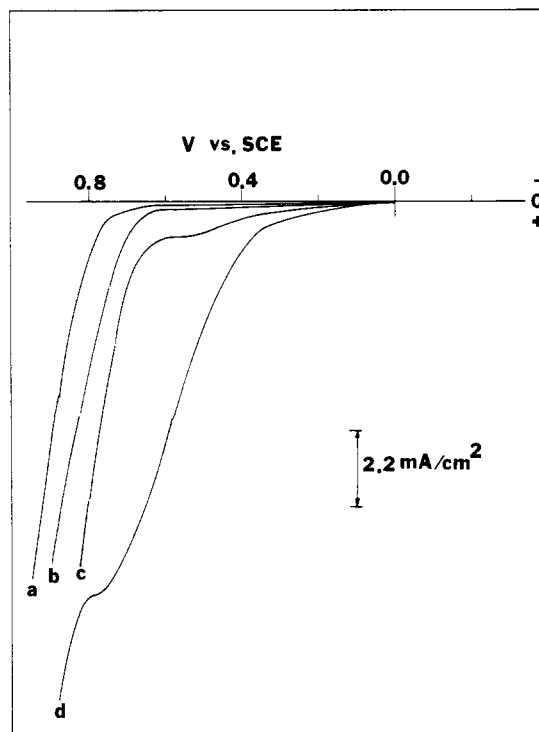
proportional to the concentration of OH$^-$, suggesting that the first wave involves the photooxidation of OH$^-$. The potential for the onset of photocurrent, V_{on}, of the first wave shifts in a negative direction by ~60 mV per pH unit; this same shift is observed in 1 M NaClO$_4$ (Figure 9). The second wave also depends strongly on pH at low pH range. Below pH 4, V_{on} shifts in a negative direction by ~60 mV per pH increment. At pH >9, the second wave becomes fairly insensitive to pH. These results suggest that these two photooxidation processes in 11 M LiCl involve the same dependent rate-determining step.[9] At high pH, the photooxidation of OH$^-$ is favored and takes place at low-bias potential. The second oxidation process can only occur when the potential of the intermediate is at a sufficiently positive potential for the oxidation

---

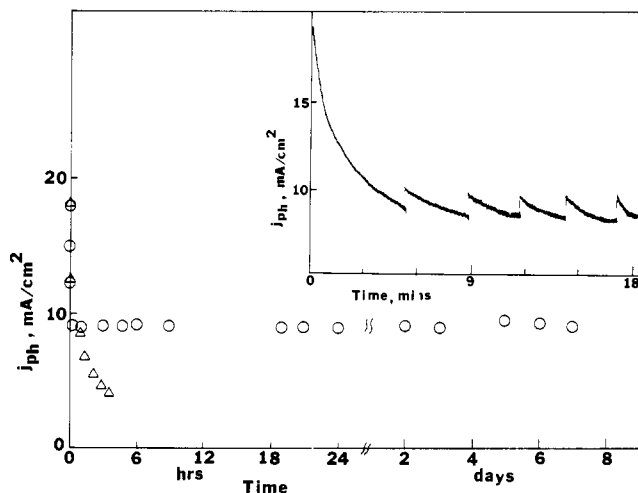(9) Trasatti, S.; O'Grady, W. E. *Adv. Electrochem. Electrochem. Eng.* **1981**, *12*, 177.

224 *J. Am. Chem. Soc., Vol. 105, No. 2, 1983*

Fan, Keil, and Bard

Figure 11. Photocurrent (at a bias potential of 1.0 V vs. SCE) vs. time. Light intensity 65 mW/cm² (tungsten–halogen lamp). $\triangle$ = n-Si(Ir) and $\bigcirc$ = n-Si(Ir)/RuO$_2$ electrodes. The insert shows the fluctuation of the photocurrent in the early stage of the test due to the buildup of Cl$_2$ gas bubbles on the electrode surface. The electrolyte solution was 11 M LiCl at pH 5.

of Cl⁻ to take place. The potential of the intermediate can apparently be increased either by consuming OH⁻ near the electrode surface or by raising the electrode potential. At low pH, the photooxidation of Cl⁻ is the dominant process. This is confirmed by the iodometric and gravimetric analyses of the oxidized products.

After long-term electrolysis of 11 M LiCl at pH 5, as shown in Figure 11, the primary gas product was identified as Cl$_2$. The coulometric efficiency of Cl$_2$ generation was higher than 90% without correction for any losses during gas collection and analysis, with the coulometric efficiency for Cl$_2$ defined as the ratio of the number of equivalent of Cl$_2$ collected to the number of faradays of photocharge passed through the PEC cell.

As shown in Figure 11, fairly durable PEC performance is observed on n-Si(Ir)/RuO$_2$ electrodes. After a total charge of ∼6000 C/cm² for 7 days of continuous illumination with a light intensity of 65 mW/cm² is passed, no appreciable degradation in photocurrent was observed. The initial current decay can be attributed to the buildup of Cl$_2$ gas bubbles on the electrode surface, since the magnitude of the photocurrent was substantially enhanced when the gas bubbles on the electrode surface were

removed by rapid stirring. This buildup of Cl$_2$ on the electrode surface enhances the back electron transfer and decreases the effective electrode area, leading to substantial decreases in the photocurrent, as shown in the insert in Figure 11. The photooxidation of H$_2$O is feasible; however, it shows the smallest V_{oc} of the redox couples studied, perhaps because of the slow kinetics of H$_2$O oxidation. Comparison of the photovoltammetric curves for H$_2$O oxidation (Figure 9) or the first wave (due to OH⁻ oxidation) with the second wave (due to Cl⁻ oxidation) in the photovoltammetric curves on n-Si(Ir)/RuO$_2$ in 11 M LiCl at high pH (Figure 10) reveals that H$_2$O or OH⁻ oxidation has a much smaller Tafel slope than Cl⁻ oxidation, especially in the low-bias potential region.

In conclusion, noble metal silicide modified n-Si electrodes have been shown to give highly stable PEC performance in aqueous solutions containing positive redox couples such as Fe$^{2+/3+}$ and Br⁻/Br$_2$. A RuO$_2$-modified n-Si(Ir) electrode can even photooxidize Cl⁻ or H$_2$O with reasonable stability. The exceptional stability and high performance of these photoelectrodes might be attributed to the following factors: (1) fast interfacial charge-transfer kinetics between the n-Si substrate and the silicides; (2) separation of the region of photocharge carrier generation (the n-Si/MSi interface) from solution contamination—this is confirmed by the photoeffect observed on a solid-state sandwich cell, Ag/n-Si(Pt)/n-Si/In-Ga, in which Ag was only partially covered on PtSi; illumination with a light intensity of 35 mW/cm² on a PtSi area that is not covered by Ag generates an open-circuit photovoltage of ∼0.3 V between the Ag and In-Ga contacts; (3) fast interfacial charge-transfer kinetics between silicide (or RuO$_2$) and solution redox species—PtSi and Pt electrodes had very similar dark electrochemical behavior, although the former usually showed slower kinetics for the redox couples studied, e.g., Fe(CN)$_6^{3-/4-}$ and methyl viologen;[10] (4) excellent adhesion of silicides on silicon substrate;[4] (5) reasonable chemical and electrochemical[10] stability of the silicides.

(10) Keil, R. G.; Bard, A. J., unpublished results.